



CHALMERS
UNIVERSITY OF TECHNOLOGY

Manipulation with Andreev states in spin active mesoscopic Josephson junctions

Downloaded from: <https://research.chalmers.se>, 2024-03-13 09:46 UTC

Citation for the original published paper (version of record):

Michelsen, J., Shumeiko, V., Wendin, G. (2008). Manipulation with Andreev states in spin active mesoscopic Josephson junctions. *Physical Review B - Condensed Matter and Materials Physics*, 77(18). <http://dx.doi.org/10.1103/PhysRevB.77.184506>

N.B. When citing this work, cite the original published paper.

Manipulation with Andreev states in spin active mesoscopic Josephson junctions

J. Michelsen, V. S. Shumeiko, and G. Wendin

Department of Microtechnology and Nanoscience, MC2, Chalmers University of Technology, SE-41296 Gothenburg, Sweden

(Received 2 October 2007; revised manuscript received 7 April 2008; published 9 May 2008)

We investigate manipulation with Andreev bound states in Josephson quantum point contacts with magnetic scattering. The Rabi oscillations in the two-level Andreev subsystems are excited by resonant driving the direction of magnetic moment of the scatterer and by modulating the superconducting phase difference across the contact. The Andreev level dynamics is manifested by the temporal oscillation of the Josephson current, which is accompanied, in the case of magnetic manipulation, also by the oscillation of the Andreev states spin polarization. The interlevel transitions obey a selection rule that forbids manipulations in a certain region of external parameters and results from specific properties of Andreev bound states in magnetic contacts: 4π periodicity with respect to the superconducting phase and strong spontaneous spin polarization.

DOI: [10.1103/PhysRevB.77.184506](https://doi.org/10.1103/PhysRevB.77.184506)

PACS number(s): 74.50.+r, 74.45.+c, 71.70.Ej

I. INTRODUCTION

Recent advances in the development and experimental investigation of nanowire based Josephson junctions^{1–3} attract new attention to the rich physics of mesoscopic Josephson effect. One of particularly interesting questions concerns the possibility to employ Josephson quantum point contacts for quantum information processing. Such contacts contain a small number of generic two-level systems—Andreev bound levels, whose quantum states can be selectively manipulated and measured.^{4,5} By modulating the phase difference across the junction, one is able to induce the Rabi oscillation in the Andreev two-level system and therefore to prepare arbitrary superposition of the Andreev states. A measurement of induced oscillation of the Josephson current allows for the Andreev level readout. Thus, the pair of Andreev bound levels belonging to the same conducting mode may serve as a quantum bit.^{6,7}

An interesting possibility to involve a spin degree of freedom in the contact quantum dynamics and to use it for qubit application has been investigated by Chtchelkatchev and Nazarov.⁸ They considered a Josephson quantum point contact with spin-orbit interaction and showed how to manipulate with the spin of the Andreev state. The properties of the Andreev bound states in spin-active mesoscopic junctions and the equilibrium Josephson effect have been extensively studied in recent literature;^{9–17} nonstationary aspects of the interaction of individual magnetic scatterers with the Josephson current have also been discussed.^{18–21}

In this paper, we investigate the methods of manipulation with the Andreev states in Josephson quantum point contacts containing a magnetic scatterer, e.g., magnetic nanoparticle situating between the superconducting electrodes.^{3,22,23} We investigate two manipulation methods: (i) time variation of the superconducting phase across the contact and (ii) time variation of the direction of magnetic moment of the scatterer. We find that in both cases, the Josephson current exhibits Rabi oscillation under the resonant drive within a certain interval of biasing superconducting phase. In the case of magnetic manipulation, the effect may only exist if the Andreev states are initially spin polarized; then, the current oscillation is accompanied by oscillation of the Andreev states

spin polarization. The phase interval, where the Rabi oscillation can be excited, decreases with increasing strength of the magnetic scatterer and eventually disappears at a large enough strength; in particular, in the π -junction regime, the Rabi oscillation is completely forbidden. This selection rule results from specific properties of the bound Andreev states in magnetic junctions as we will show.

For a static scatterer, the spin rotation symmetry around the direction of its magnetic moment is preserved. This allows for the contact description in terms of a two-component Nambu spinor,²⁴ which is similar to nonmagnetic junctions, thus avoiding a double counting problem. Within such an approach, the two bound Andreev levels per conducting modes are only relevant, giving a complete quantitative description of the stationary Josephson effect as well as the resonant two-level transitions and nonstationary current response under the phase manipulation.⁶ Consideration of the spin conjugated Nambu spinor gives a completely equivalent physical description in terms of a reciprocal pair of Andreev bound states; both of the pictures mirror each other.

Time variation of the direction of the magnetic moment of the scatterer leads to a violation of the spin rotation symmetry and induces coupling between the spin conjugated Nambu spinors. This results in a unitary rotation in the extended space of the four Andreev bound states. It turns out, however, that this rotation splits into two equivalent rotations in invariant two-level subspaces, which mirror each other. Thus, the contact response in this case can also be explained in terms of the two-level Rabi dynamics. For the two different ways of magnetic manipulation considered—instant switching and small-amplitude resonant oscillation of the direction of the magnetic moment of the scatterer, the Andreev two-level dynamics has a physical meaning of precession and nutation of the spin polarization of the Andreev levels, respectively. Thus, the spin polarization of Andreev states is required in order to observe a nontrivial dynamical response.⁸ Such a possibility naturally exists, as we will show, in the contact under consideration: the equilibrium Andreev states exhibit strong spin polarization, up to the maximum values of $\pm 1/2$ at low temperature, in certain regions of the superconducting and Zeeman phases.

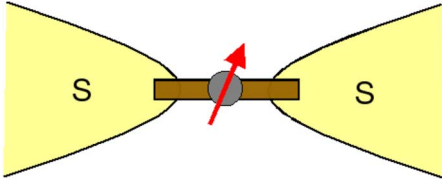


FIG. 1. (Color online) Sketch of a magnetic Josephson point contact: superconducting reservoirs are connected by a nanowire of length L smaller than the coherence length and a magnetic nanoparticle creates a local classical magnetic field.

II. CONTACT DESCRIPTION

Consider a one-mode quantum point contact with superconducting electrodes connected by a normally conducting nanowire, as shown in Fig. 1. The left and right electrodes (L, R) are described with the BCS Hamiltonian,

$$H_S = \int_{L,R} dx \sum_{\sigma=\uparrow,\downarrow} \hat{\psi}_{\sigma}^{\dagger}(x) \left(\frac{p^2}{2m} - \mu(x,t) \right) \hat{\psi}_{\sigma}(x) + \Delta^*(x,t) \hat{\psi}_{\uparrow}(x) \hat{\psi}_{\downarrow}(x) + \Delta(x,t) \hat{\psi}_{\downarrow}^{\dagger}(x) \hat{\psi}_{\uparrow}^{\dagger}(x). \quad (1)$$

Aiming to investigate the effect of time variation of the superconducting phase difference φ across the junction, we consider the order parameter that has the form $\Delta(x,t) = \Delta e^{i\varphi(x,t)/2}$ and $\varphi(x,t) = \varphi(t) \text{sgn } x$ and the electrochemical potential, $\mu(x,t)$, which has the form $\mu(x,t) = E_F - \hbar \partial_t \varphi / 2$, which provides the electroneutrality condition within the electrodes.⁷

To explore the spin properties of the Andreev states, we assume that the contact nanowire contains a magnetic scatterer, e.g., magnetic nanoparticle (Fig. 1). We assume for simplicity that the magnetic field $\mathbf{H}(x,t)$ induced by the scatterer is localized within the nanowire on a distance l smaller than the distance L between the electrodes, thus not affecting the superconductivity within the electrodes; furthermore, we will treat this magnetic field as a given external parameter, neglecting the back action effect from the current. Then, the Hamiltonian of the normal region of the junction has the form

$$H_N = \int_{-L/2}^{L/2} dx \sum_{\sigma\sigma'} \hat{\psi}_{\sigma}^{\dagger}(x) \left[\left(\frac{p^2}{2m} - E_F + U(x) \right) \delta_{\sigma\sigma'} + \frac{1}{2} \mu_B \boldsymbol{\sigma}_{\sigma\sigma'} \cdot \mathbf{H}(x,t) \right] \hat{\psi}_{\sigma'}(x), \quad (2)$$

where $U(x)$ is the scalar potential of the scatterer. We assume symmetric with respect to $x=0$ spatial distributions of the scalar potential and the magnetic field and also a fixed direction of the magnetic field, which will vary with time during the manipulation.

In the stationary case, the Hamiltonian (2) preserves the spin rotational symmetry around the direction of the magnetic field. By choosing the spin quantization axis along this direction, we describe the electron propagation through the normal region of the junction with a transfer matrix T_e ,

$$T_e = \hat{d}^{-1} \begin{pmatrix} e^{i\sigma_z(\beta/2)} & i\hat{r} \\ -i\hat{r} & e^{-i\sigma_z(\beta/2)} \end{pmatrix}, \quad (3)$$

where $\hat{d} = \text{diag}(d_{\uparrow}, d_{\downarrow})$ and $\hat{r} = \text{diag}(r_{\uparrow}, r_{\downarrow})$. Contact description in terms of the spin active scattering matrix has been extensively discussed in literature.^{11,25} The impurity scalar potential produces spatially symmetric scattering with transmission amplitudes, $d_{\uparrow}, d_{\downarrow}$, and reflection amplitudes, $r_{\uparrow}, r_{\downarrow}$, which may be different for different spin orientations (spin selection). The scattering phase shift β between the opposite spin orientations is induced by the Zeeman effect,

$$\beta = \frac{\mu_B H l}{\hbar v_F}. \quad (4)$$

The physical observables of interest, i.e., the Josephson current and spin polarization, are described with a single electron density matrix $\rho(x, x', t)$ associated with a two-component Nambu field²⁶ $\Psi(x, t)$,

$$\Psi(x, t) = \begin{pmatrix} \hat{\psi}_{\uparrow}(x, t) \\ \hat{\psi}_{\downarrow}^{\dagger}(x, t) \end{pmatrix}, \quad \rho(x, x', t) = \langle \Psi(x, t) \Psi^{\dagger}(x', t) \rangle \quad (5)$$

(here, the angular brackets indicate statistical averaging). An alternative description is given by a density matrix, $\tilde{\rho}(x, x', t)$, associated with the spin conjugated Nambu field, $\tilde{\Psi}(x, t)$,

$$\tilde{\Psi}(x, t) = \begin{pmatrix} \hat{\psi}_{\downarrow}(x, t) \\ -\hat{\psi}_{\uparrow}^{\dagger}(x, t) \end{pmatrix}, \quad \tilde{\rho}(x, x', t) = \langle \tilde{\Psi}(x, t) \tilde{\Psi}^{\dagger}(x', t) \rangle. \quad (6)$$

The two Nambu fields are connected via a fundamental symmetry relation imposed by the singlet nature of the BCS pairing,

$$\tilde{\Psi}(x, t) = i\sigma_y (\Psi^{\dagger})^T. \quad (7)$$

In what follows, we will use these two reciprocal representations, i.e., ϕ representation and $\tilde{\phi}$ representation, respectively (see Appendix B). This will allow us to avoid the redundancy, which is introduced by Eq. (7), of a commonly used four-component Nambu formalism^{9-14,16} and to explicitly show that the stationary Josephson effect as well as nonstationary response to the phase manipulation can be fully understood within the framework of the two bound Andreev states per conducting mode associated with either of these two reciprocal representations.

III. ANDREEV STATE SUBSYSTEM

In this section, we outline the properties of the stationary Andreev states, which are of importance for the discussion of nonstationary effects. The details of derivations are presented in Appendix A.

Within the two-component Nambu formalism,²⁶ the quasiparticle states in the stationary contact are given by the Bogoliubov–de Gennes equation,

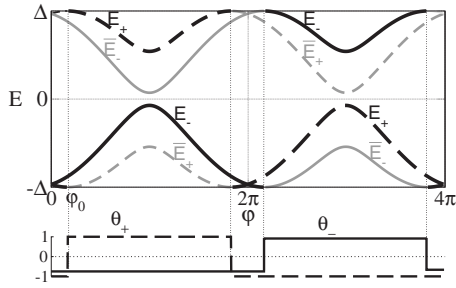


FIG. 2. Andreev level energy spectrum for $\sin(\beta/2) < \sqrt{D}$ ($D = 0.9, \beta = 0.5$). Upper panel: θ functions, as shown in the lower panel, define the spectrum discontinuity points at $2\pi n \pm \varphi_0$. The vertical dotted lines separate the regions of weak and strong Zeeman effects.

$$h\phi = E\phi, \quad h = (p^2/2m - E_F)\sigma_z + \Delta\sigma_x, \quad (8)$$

which is supplemented with the boundary condition at the contact, which for a short contact is given by the transfer matrix, $T = \exp(i\sigma_z\varphi/2)T_e$ [Eq. (A3)]. The energy spectrum of the bound states consists of the two levels according to Eq. (A9),

$$E_s = \theta_s \Delta \cos(s\eta - \beta/2), \quad s = \pm, \quad (9)$$

where $\theta_s = \text{sgn}[\sin(s\eta - \beta/2)]$ and the parameter η is defined through $\sin \eta = \sqrt{D} \sin(\varphi/2)$, where D is the contact transparency. This energy spectrum is asymmetric with respect to the chemical potential, $E=0$, and is 4π periodic with respect to the phase difference, as shown in Fig. 2, the spectral branches cross at $\varphi = 2\pi n$. In Fig. 2, the energy levels of a reciprocal Andreev level pair, $\tilde{E}_s = -E_s$, are also shown, whose wave functions, $\tilde{\phi}_s = (i\sigma_y)\phi_s^*$, are associated with the spin conjugated Nambu field [Eq. (6)] ($\tilde{\phi}$ representation, see Appendix B).

The reason for the 4π periodicity and the level crossings is the symmetry of the problem, which is reflected in the property [Eq. (A12)]. By introducing the parity operator P that permutes the wave functions at the left and right sides of the junction, $P\phi(x < 0) = \phi(x > 0)$, we write Eq. (A12) in the following form:²⁷

$$\hat{\Lambda}\hat{\phi}_s(x) = s\theta_s\hat{\phi}_s(x), \quad \hat{\Lambda} = P \begin{pmatrix} -\sigma_x & 0 \\ 0 & \sigma_x \end{pmatrix}. \quad (10)$$

According to this equation, the Andreev level wave functions are simultaneously the eigenfunctions of the symmetry operator $\hat{\Lambda}$ with eigenvalues $s\theta_s$. Furthermore, the energy branches, E_- and E_+ , in the neighboring phase intervals in Fig. 2 correspond to the different eigenvalues of the operator $\hat{\Lambda}$. The properties of the Andreev states are therefore qualitatively different within the phase intervals, where $\theta_s = \theta_{-s}$ and $\theta_s = -\theta_{-s}$. To emphasize the difference, we will refer to the former ones as the regions of strong Zeeman effect (ZE), $\sin \beta/2 > \sqrt{D} \sin \varphi/2$, and the latter ones as the regions of weak ZE, $\sin \beta/2 < \sqrt{D} \sin \varphi/2$. These regions are separated by the points where the energy levels touch the continuum, $\varphi = 2\pi n \pm \varphi_0$, $\varphi_0 = 2 \arcsin(1/\sqrt{D} \sin \beta/2)$. At a sufficiently large Zeeman phase, $\sin \beta/2 > \sqrt{D}$, the weak ZE regions dis-

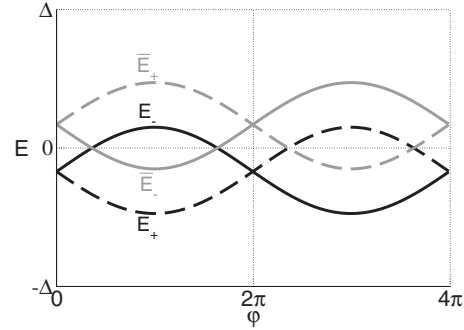


FIG. 3. Andreev level energy spectrum for $\sin(\beta/2) > \sqrt{D}$ ($D = 0.1, \beta = 2.8$). The strong ZE region spreads over whole phase axis.

appear, while the strong ZE regions spread over the whole superconducting phase axis. The bound energy levels, $E_{\pm}(\varphi)$, depart from the continuum forming “cigars” (see Fig. 3); they belong to the orthogonal eigensubspaces of the operator $\hat{\Lambda}$ at all phases. The π contact is realized in this regime, at $\beta = \pi$,²⁸ when the reciprocal cigars coincide and symmetrically situate with respect to $E=0$.

A qualitative difference between the regions of strong and weak ZEs is illustrated by the properties of the Josephson current. Starting with a general expression for the charge current through the density matrix,

$$I(t) = \frac{e\hbar}{2mi} (\partial_x - \partial_{x'}) [\partial(x - x') - \text{Tr} \rho(x, x', t)]_{x=x'=0}, \quad (11)$$

we truncate it to the Andreev level subspace,

$$I_A(t) = \sum_{ss'} I_{ss'} \left(\frac{1}{2} \delta_{s's} - \rho_{s's}(t) \right). \quad (12)$$

Here,

$$\rho_{ss'}(t) = \langle \phi_s | \rho(t) | \phi_{s'} \rangle = \int dx dx' \text{Tr} [\rho(x, x', t) \phi_{s'}(x') \phi_s^\dagger(x)] \quad (13)$$

is the density matrix in the Andreev level representation [Eqs. (A11) and (A12)]; the trace refers to the electron-hole space. The current matrix $I_{ss'}$ reads

$$I_{ss'} = \frac{2e}{\hbar} \left[\begin{pmatrix} \partial_\varphi E_+ & 0 \\ 0 & \partial_\varphi E_- \end{pmatrix} + (1 - \theta_s \theta_{-s}) \sqrt{RD} \sin \frac{\varphi}{2} \frac{\sqrt{\xi_+ \xi_-}}{2\varepsilon} \begin{pmatrix} 0 & 1 \\ 1 & 0 \end{pmatrix} \right]. \quad (14)$$

The diagonal elements give the expectation values of the currents of Andreev states, while the off-diagonal part describes the current quantum fluctuation.⁷ The off-diagonal part is finite in the weak ZE regions, where $\theta_s \theta_{-s} = -1$, while it is zero in the strong ZE regions. This implies that the current quantum fluctuation is fully suppressed in the strong ZE regions: here, the current matrix commutes with the Andreev level Hamiltonian, which is diagonal in this representation $h_{ss'} = \delta_{ss'} E_s$.

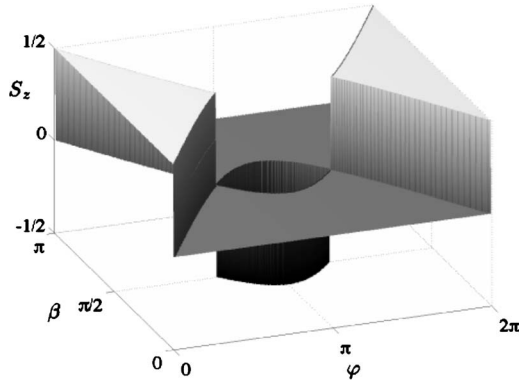


FIG. 4. Equilibrium spin polarization of Andreev levels at zero temperature and at $D > 1/2$; the central region with $S = -1/2$ emerges at $D = 1/2$ at $\varphi = \pi, \beta = \pi/2$ and grows with D , reaching the lines $\beta = 0$ and $\beta = \pi$ at $D = 1$.

In the equilibrium, $\rho_{ss'} = \delta_{ss'} n_F(-E_s)$ and the Andreev current in Eq. (12) takes the form

$$I_A = -\frac{e\Delta}{\hbar} \sum_s \partial_\varphi E_s \tanh(E_s/2T). \quad (15)$$

One can confirm by direct calculation that the current of the continuum states vanishes, thus Eq. (15) represents the total Josephson current. This equation coincides with the result obtained by using the four-component Nambu formalism,^{9-14,16} and it can also be obtained by working with the reciprocal Nambu representation by using Eq. (B9).

The spin polarization of the Andreev states plays an important role in magnetic manipulation. The asymmetry of the Andreev spectrum with respect to the zero energy together with the spectrum discontinuities result in a peculiar phase dependence of the spin polarization of Andreev levels. The z component of electronic spin density in the contact is given by

$$S(x, t) = \frac{1}{2} [\delta(x - x') - \text{Tr} \rho(x, x', t)]_{x=x'}. \quad (16)$$

By truncating this equation to the Andreev level subspace and by integrating over x and using normalization condition for the bound state wave functions, we find the spin polarization of the Andreev level pair,

$$S_A = (1/2)(1 - f_+ - f_-), \quad (17)$$

where $f_s = \rho_{ss}$ are the population numbers.

Thus, the spin polarization of the Andreev levels is entirely determined by their (generally nonequilibrium) population numbers: For an empty Andreev level pair, $f_\pm = 0$, the spin polarization is $S = 1/2$, while for fully populated levels, $f_\pm = 1$, it is $S = -1/2$. For the single particle occupation of the level pair, $f_+ + f_- = 1$, the spin polarization is zero, $S = 0$. In nonmagnetic contacts, the equilibrium spin polarization of Andreev levels is always zero, $S = 0$, by virtue of the identity, $n_F(-E_+) + n_F(-E_-) = 1$, that holds due to the spectrum symmetry, $E_+ = -E_-$. In magnetic contacts, the spin polarization sharply varies in the φ - β parameter plane (see Fig. 4). At zero temperature, $f_s = \theta(E_s)$, the spin polarization is zero in

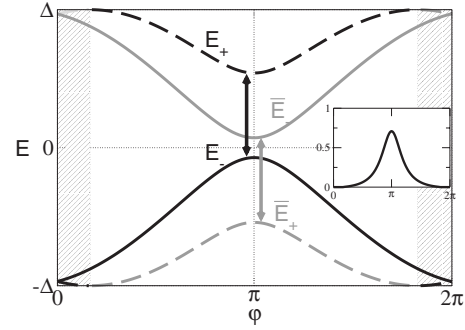


FIG. 5. Interlevel transitions induced by time oscillation of the phase difference; the shadow regions indicate the forbidden regions; transitions in $\tilde{\phi}$ representation (reduced-intensity lines) are equivalent to the transitions in ϕ representation (full-intensity lines); $D = 0.9$ and $\beta = 0.5$. Inset: transition matrix element as function of φ .

the regions bound by the lines, $\sin(\varphi/2) = \sin(\beta/2)/\sqrt{D}$ and $\sin(\varphi/2) = \cos(\beta/2)/\sqrt{D}$; the first region corresponds to a weak ZE. Outside these regions, the Andreev levels are strongly polarized, $S = 1/2$. At small contact transparencies, $D < 1/2$, the above mentioned lines do not overlap, while at $D > 1/2$ they do, forming an island of strong negative polarization, $S = -1/2$, around the point, $\varphi = \pi, \beta = \pi/2$ (see Fig. 4). This island grows with increasing transparency, eventually touching the lines, $\beta = 0$ and $\beta = \pi$, at $D = 1$.

In contrast to the charge density, the spin density in Eq. (16) obeys the conservation equation, $\partial_t S(x, t) + \partial_x I_S(x, t) = 0$. The consequence of this is the zero spin current of the Andreev states, $I_{SA} = 0$: under the stationary condition, the partial spin current of the Andreev state must be constant in space, and being proportional to the bound wave function, it vanishes at infinity; thus, it is identically equal to zero.²⁹

IV. PHASE MANIPULATION

Now, we turn to the discussion of the Andreev level dynamics under the time-dependent phase. Similar to nonmagnetic junctions this dynamics involve only the bound levels belonging to the same Nambu representation,⁴⁻⁶ as shown in Fig. 5. The frequency of the phase time variation must be small compared to the distance to the gap edges to prevent the level-continuum transitions, $\omega \ll \Delta - |E_s|$.

The time evolution of the contact density matrix, $\rho(t)$, is governed by the Liouville equation, $i\hbar \partial_t \rho = [H, \rho]$, with the Hamiltonian of Eq. (8), which is supplemented with the non-stationary boundary condition, $T = \exp[i\sigma_z \varphi(t)/2] T_e$. Now, we truncate the density matrix using the instantaneous Andreev eigenfunctions, $\phi_s[\varphi(t)]$ [cf. Eq. (13)],

$$\rho_{ss'}(t) = \langle \phi_s(t) | \rho(t) | \phi_{s'}(t) \rangle. \quad (18)$$

This density matrix obeys the Liouville equation $i\hbar \partial_t \rho = [H, \rho]$ with a truncated Hamiltonian, which in this basis is given by

$$H_{ss'} = \langle \phi_s | h | \phi_{s'} \rangle - \langle \phi_s | i\hbar \partial_t | \phi_{s'} \rangle = E_s \delta_{ss'} - \hbar \dot{\varphi} \langle \phi_s | i\partial_\varphi | \phi_{s'} \rangle, \quad (19)$$

where $E_s[\varphi(t)]$ and $\phi_s[\varphi(t)]$ are given by Eqs. (A9), (A11), and (A12), respectively.

The matrix element, $\langle \phi_s | i\partial_\varphi | \phi_{s'} \rangle$, is found to be zero for $s'=s$, while for the interlevel transitions, $s'=-s$, it reads

$$\langle \phi_s | i\partial_\varphi | \phi_{-s} \rangle = is(1 - \theta_s \theta_{-s}) \frac{\Lambda(\varphi)}{2},$$

$$\Lambda(\varphi) = \frac{\sqrt{RD}}{2} \sin^2 \frac{\varphi}{2} \frac{\sqrt{\zeta_+ \zeta_-}}{\varepsilon^2(\zeta_+ + \zeta_-)}. \quad (20)$$

From this, we find that in the weak ZE regions, $\theta_s \theta_{-s} = -1$, the nonstationary Andreev level Hamiltonian has the form

$$H(t) = \begin{pmatrix} E_+ & 0 \\ 0 & E_- \end{pmatrix} + \hbar \dot{\varphi} \Lambda(\varphi) \begin{pmatrix} 0 & -i \\ i & 0 \end{pmatrix}, \quad \sqrt{D} \sin \frac{\varphi}{2} > \sin \frac{\beta}{2}. \quad (21)$$

This equation provides generalization to a magnetic junction of the Hamiltonian derived in Ref. 6: the level coupling coincides with the one in nonmagnetic junction when $\beta=0$ and remains finite when $\beta \neq 0$ but only inside the weak ZE region, decreasing toward the edges of this region (see inset in Fig. 5). In the strong ZE region, the matrix element is identically zero ($\theta_s \theta_{-s} = +1$), and the Hamiltonian is diagonal,

$$H(t) = \begin{pmatrix} E_+ & 0 \\ 0 & E_- \end{pmatrix}, \quad \sqrt{D} \sin \frac{\varphi}{2} < \sin \frac{\beta}{2}. \quad (22)$$

Thus, we conclude that no operation with Andreev levels is possible in the strong ZE regime.

Equation (21) is convenient for the calculation of Rabi oscillation in the Andreev level system under the resonant driving, $\varphi(t) = \varphi + \delta \sin \omega t$, where $\omega = (E_+ - E_-)/\hbar$. By inserting this in Eq. (21), we get

$$H = \frac{\hbar \omega}{2} \sigma_z + \hbar \Lambda \delta \omega \cos \omega t \sigma_y. \quad (23)$$

By assuming a small amplitude of the phase oscillation, $\delta \ll 1$, and by using the rotating wave approximation, we find the time-dependent density matrix in the rotating frame,

$$\rho(t) = \rho(0) - \frac{f_+(0) - f_-(0)}{2} (1 - \cos \Lambda \delta \omega t - \sin \Lambda \delta \omega t \sigma_x), \quad (24)$$

where $\rho(0) = \text{diag}(f_+(0), f_-(0))$. The Rabi oscillation of the Andreev levels generates a time-dependent Josephson current,

$$I(t) = I(0) - \frac{2e}{\hbar} [f_+(0) - f_-(0)] \sin^2 \frac{\Lambda \delta \omega t}{2} \sum_s \partial_\varphi E_s. \quad (25)$$

The Rabi oscillation [Eq. (24)] and the time oscillation of the Josephson current [Eq. (25)] vanish if the Andreev levels are initially fully spin polarized, $S(0) = \pm 1/2$, since $f_+(0) = f_-(0)$ in this case. Thus, an additional requirement for the

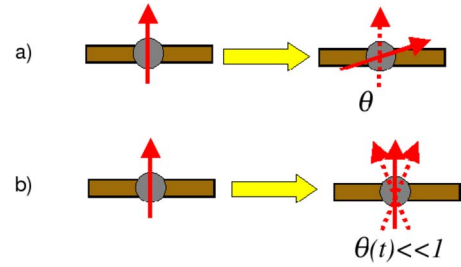


FIG. 6. (Color online) Sketch of manipulation with magnetic field. (a) Instant switching of direction of magnetic field. (b) Small-amplitude oscillation of magnetic field with resonant frequency (electron spin resonance).

phase manipulation is to bias the contact in the region outside the negative-spin island in Fig. 4.

V. SPIN MANIPULATION

Now, we proceed with the discussion of the spin manipulation. We consider the two ways of driving Andreev level spin, which are presented in Fig. 6: (i) rapid change of the *direction* of the magnetic moment of the scatterer (dc pulsing) and (ii) harmonic oscillation with resonance frequency of the magnetic moment direction (rf pulsing). In both cases, the spin rotation symmetry is violated; therefore, the junction dynamics cannot be described with only one Nambu pseudospinor but involves both the spin conjugated Nambu pseudospinors. The interlevel transitions in this case physically describe a rotation of the Andreev level spin.

A. dc pulsing

Suppose the Andreev levels are initially prepared in a stationary state with nonzero spin, which points along the applied magnetic field (z axis). Such states were discussed in Secs. II and III. Let us now suppose that the magnetic field is rapidly rotated by an angle θ around the y axis, as shown in Fig. 6(a). Such a manipulation is described by the rotation of the electronic T matrix in Eq. (3),

$$T_e \rightarrow UT_e U^\dagger, \quad U = \begin{pmatrix} \cos \frac{\theta}{2} & \sin \frac{\theta}{2} \\ -\sin \frac{\theta}{2} & \cos \frac{\theta}{2} \end{pmatrix}, \quad (26)$$

and it mixes the Nambu pseudospinors Ψ and $\tilde{\Psi}$. To describe the effect of this manipulation, we introduce the extended four-component Nambu space, $(\Psi, \tilde{\Psi})^T$, and the corresponding single particle density matrix,

$$\Pi(x, x', t) = \begin{pmatrix} \langle \Psi(x, t) \Psi^\dagger(x', t) \rangle & \langle \Psi(x, t) \tilde{\Psi}^\dagger(x', t) \rangle \\ \langle \tilde{\Psi}(x, t) \Psi^\dagger(x', t) \rangle & \langle \tilde{\Psi}(x, t) \tilde{\Psi}^\dagger(x', t) \rangle \end{pmatrix}. \quad (27)$$

This density matrix operates in the Hilbert space spanned by the extended eigenbasis,

$$\Phi_\nu(x) = \begin{pmatrix} \phi_\nu(x) \\ 0 \end{pmatrix}, \quad \Phi_{\tilde{\nu}}(x) = \begin{pmatrix} 0 \\ \tilde{\phi}_\nu(x) \end{pmatrix}. \quad (28)$$

The transformation U induces rotation of the extended basis,

$$\Phi_\alpha(x) \rightarrow U\Phi_\alpha(x), \quad \alpha \in \{\nu, \tilde{\nu}\}. \quad (29)$$

The eigenenergies, however, remain the same since such a rotation just corresponds to changing the spin quantization axis.

The wave functions [Eq. (28)] form a complete set in the extended space, and thus, any operator can be expressed through them,

$$A(x, x') = \sum_{\alpha, \beta} \Phi_\alpha(x) \Phi_\beta^\dagger(x') A_{\alpha\beta}. \quad (30)$$

In particular, for a stationary system with a spin rotational invariance, we have for the density matrix,

$$\Pi(x, x') = \sum_\alpha \Phi_\alpha(x) \Phi_\alpha^\dagger(x') f_\alpha, \quad (31)$$

and the Hamiltonian,

$$H(x) = \sum_\alpha \Phi_\alpha(x) \Phi_\alpha^\dagger(x) E_\alpha. \quad (32)$$

However, one has to remember that this description is redundant, and rigorous constraints hold in the occupation numbers, $\tilde{f}_\nu = 1 - f_\nu$, and eigenenergies, $\tilde{E}_\nu = -E_\nu$.

We now write down the Hamiltonian after the magnetic field rotation in the form

$$H(x) = \sum_\alpha U \Phi_\alpha(x) E_\alpha \Phi_\alpha^\dagger(x) U^\dagger, \quad t > 0. \quad (33)$$

In the initial basis, this Hamiltonian is represented with the matrix,

$$H_{\alpha\beta} = \sum_\mu \langle \Phi_\alpha | U | \Phi_\mu \rangle E_\mu \langle \Phi_\mu | U^\dagger | \Phi_\beta \rangle, \quad t > 0, \quad (34)$$

or explicitly,

$$\begin{aligned} H_{\nu\nu'} &= \cos^2 \frac{\theta}{2} E_\nu \delta_{\nu\nu'} - \sin^2 \frac{\theta}{2} \sum_{\mu \neq \nu, \nu'} \langle \phi_\nu | \tilde{\phi}_\mu \rangle E_\mu \langle \tilde{\phi}_\mu | \phi_{\nu'} \rangle, \\ H_{\tilde{\nu}\tilde{\nu}'} &= -\cos^2 \frac{\theta}{2} E_\nu \delta_{\nu\nu'} + \sin^2 \frac{\theta}{2} \sum_{\mu \neq \nu, \nu'} \langle \tilde{\phi}_\nu | \phi_\mu \rangle E_\mu \langle \phi_\mu | \tilde{\phi}_{\nu'} \rangle, \\ H_{\nu\tilde{\nu}'} &= -\sin \theta \langle \phi_\nu | \tilde{\phi}_{\nu'} \rangle \frac{E_\nu + E_{\nu'}}{2}. \end{aligned} \quad (35)$$

Here, the orthogonality relations were used, $\langle \phi_\nu | \phi_\mu \rangle = \langle \tilde{\phi}_\nu | \tilde{\phi}_\mu \rangle = \delta_{\mu\nu}$ and $\langle \phi_\nu | \phi_{\tilde{\nu}} \rangle = 0$, Eq. (B5).

At this point, we restrict ourselves to the Andreev level subspace and present the truncated Hamiltonian in the following form (by using the symmetries $E_s = -\tilde{E}_s$ and $\langle \phi_+ | \tilde{\phi}_- \rangle = -\langle \phi_- | \tilde{\phi}_+ \rangle$):

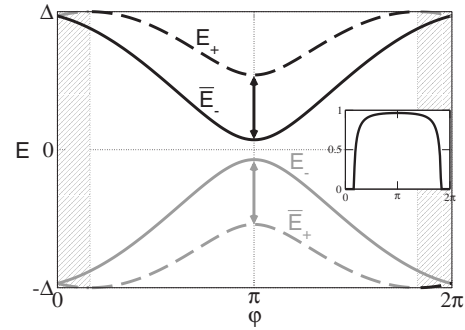


FIG. 7. Interlevel transitions induced by magnetic manipulation; the shadow regions indicate the forbidden regions; transitions between the levels (E_-, \tilde{E}_+) (reduced-intensity lines) are equivalent to the transitions (E_+, \tilde{E}_-) (full-intensity lines); $D=0.9$ and $\beta=0.5$. Inset: transition matrix element as a function of φ .

$$H^{(4)} = \begin{pmatrix} E_0 + W & 0 & 0 & V \\ 0 & -E_0 + W & -V & 0 \\ 0 & -V & -E_0 - W & 0 \\ V & 0 & 0 & E_0 - W \end{pmatrix}, \quad (36)$$

where

$$\begin{aligned} E_0, W &= \left(\cos^2 \frac{\theta}{2} - \sin^2 \frac{\theta}{2} |M|^2 \right) \frac{E_+ + E_-}{2}, \\ V &= -M \sin \theta \frac{E_+ + E_-}{2}, \end{aligned} \quad (37)$$

and the interlevel matrix element,

$$M = \langle \phi_+ | \tilde{\phi}_- \rangle = (\theta_s - \theta_{-s}) \cos \frac{\beta}{2} \frac{\sqrt{\zeta_+ \zeta_-}}{\zeta_+ + \zeta_-}. \quad (38)$$

The matrix element (38) equals to zero in the strong ZE region ($\theta_s = \theta_{-s}$); thus, the manipulation does not produce any effect there, which is similar to the phase manipulation [see the inset in Fig. 7].

The Hamiltonian (36) has a block-diagonal form, describing identical rotations in the two orthogonal subspaces, which are spanned by the eigenvectors $(\phi_+, \tilde{\phi}_-)$ and $(\phi_-, \tilde{\phi}_+)$. Thus, the problem reduces to solving for two physically equivalent two-level systems. By choosing the subspace $(\phi_+, \tilde{\phi}_-)$, we have the two-level Hamiltonian,

$$H^{(2)} = \begin{pmatrix} W & V \\ V & -W \end{pmatrix}. \quad (39)$$

By introducing the projection operators on the eigensubspaces,

$$H^{(2)} = \sum_{\lambda=\pm} \lambda \hbar \Omega P_\lambda, \quad P_\lambda = \frac{1}{2} \left(1 + \lambda \frac{\sigma_z W + \sigma_x V}{\hbar \Omega} \right),$$

$$\hbar\Omega = \sqrt{W^2 + V^2} = \frac{(E_+ + E_-)}{2} \left(\cos^2 \frac{\theta}{2} + \sin^2 \frac{\theta}{2} |M|^2 \right), \quad (40)$$

where $\lambda\hbar\Omega$ are the eigenenergies, we have for the time evolution of the two-level density matrix,

$$\Pi^{(2)}(t) = e^{-i(Ht/\hbar)} \Pi^{(2)}(0) e^{i(Ht/\hbar)} = \sum_{\lambda\lambda'} e^{i(\lambda' - \lambda)\Omega t} P_\lambda \Pi^{(2)}(0) P_{\lambda'}. \quad (41)$$

By assuming the initial density matrix to be stationary (not necessarily equilibrium) and by expressing it through the level occupation numbers of the ϕ representation,

$$\Pi^{(2)}(0) = \begin{pmatrix} f_+(0) & 0 \\ 0 & 1 - f_-(0) \end{pmatrix}, \quad (42)$$

we obtain

$$\begin{aligned} \Pi^{(2)}(t) &= \Pi^{(2)}(0) + 2S_A(0) \begin{pmatrix} |a(t)|^2 & b(t) \\ b(t)^* & -|a(t)|^2 \end{pmatrix}, \\ a(t) &= -i \frac{V}{\hbar\Omega} \sin \Omega t, \quad b(t) = a(t) \left[\cos \Omega t + i \frac{W}{\hbar\Omega} \sin \Omega t \right], \end{aligned} \quad (43)$$

where $S_A(0) = (1/2)[1 - f_+(0) - f_-(0)]$ is the initial spin polarization of the Andreev levels, as given by Eq. (17). Thus, no rotation is induced for spin unpolarized Andreev levels. Furthermore, the frequency of the rotation is proportional to the level splitting, $\hbar\Omega \propto E_+ - \tilde{E}_- = E_+ + E_-$, i.e., to the magnetic field.

The time evolution of the occupation numbers $f_s(t)$ of the Andreev levels in the ϕ representation is extracted from Eq. (43),

$$f_s(t) = f_s(0) + 2S_A(0) \frac{V^2}{(\hbar\Omega)^2} \sin^2 \Omega t. \quad (44)$$

This relation illustrates the nonunitary evolution of the Andreev levels in this representation, $f_+(t) + f_-(t) \neq \text{const.}$ Equation (44) allows us to obtain the time dependence of the spin polarization of the Andreev levels,

$$S_A(t) = \frac{1}{2}[1 - f_+(t) - f_-(t)] = S_A(0) \left(1 - \frac{2V^2}{(\hbar\Omega)^2} \sin^2 \Omega t \right). \quad (45)$$

To calculate the Josephson current, we use the expression through the current matrix in the ϕ representation [Eqs. (12) and (14)],

$$I(t) = \sum_{ss'} I_{ss'} \left(\frac{1}{2} \delta_{s's} - \rho_{s's}(t) \right). \quad (46)$$

The diagonal elements of the density matrix ρ_{ss} are given by Eq. (44). On the other hand, the off-diagonal elements $\rho_{ss'}$ equal zero because the spin manipulation does not induce transitions between the eigenstates of the same (either ϕ or $\tilde{\phi}$) representation. Therefore,

$$I(t) = \frac{2e}{\hbar} \sum_s \partial_\phi E_s f_s(t) = I(0) + \frac{4e}{\hbar} S_A(0) \frac{V^2}{(\hbar\Omega)^2} \sin^2 \Omega t \sum_s \partial_\phi E_s. \quad (47)$$

In summary, the conditions for the observation of the non-stationary contact response, biasing in a weak ZE region with a finite spin polarization, can be only fulfilled in the central island region in Fig. 4 with negative polarization. This constraint can be relaxed by pumping the initial level populations away from equilibrium, as suggested in Ref. 8.

To conclude this section, we note that the dc pulsing of the magnetic field does not allow one to reach every point on the Bloch sphere: this is due to the fact that U is not an invariant operation on the Andreev level subspace of the extended Nambu space, which physically means a leakage to the continuum (similar effect exists also for the phase manipulation with dc pulses³⁰). However, for small rotation angles and not close to the edges of the weak ZE region, the matrix element M is close to unity, and the leakage is small; it can be further reduced by using rapid adiabatic change of the magnetic field, i.e., rapid on the time scale of the Andreev level splitting but slow on the time scale of the distance of the Andreev levels to the continuum. This shortcoming does not exist for the resonant rf pulsing.

B. rf pulsing

Now, let us consider a time-dependent rotation of the magnetic field,

$$T \rightarrow U[\theta(t)] T U^\dagger[\theta(t)],$$

where $\theta(t)$, as before, is the angle of rotation around the y axis [see Fig. 6(b)]. We can now define the instantaneous eigenstates as

$$U(t) \Phi_\alpha(x), \quad (48)$$

satisfying the instantaneous boundary condition [Eq. (3)], with $T_e \rightarrow U T_e U^\dagger$. The time-dependent Hamiltonian can then be written similar to Eq. (33),

$$H(x, t) = \sum_\alpha U(t) \Phi_\alpha(x) E_\alpha \Phi_\alpha^\dagger(x) U^\dagger(t). \quad (49)$$

Since the energy eigenvalues do not depend on the direction of the quantization axis, they remain time independent. Now, similar to Eq. (31), we can expand the density matrix in terms of these instantaneous eigenfunctions,

$$\Pi(x, x', t) = \sum_{\alpha, \beta} U(t) \Phi_\alpha(x) \Phi_\beta^\dagger(x') U^\dagger(t) \Pi_{\alpha\beta}(t). \quad (50)$$

The matrix $\Pi_{\alpha\beta}(t)$ satisfies the Liouville equation with the Hamiltonian

$$\begin{aligned} H_{\alpha\beta}(t) &= \int dx \Phi_\alpha^\dagger(x) U^\dagger(t) [H(x) - i\hbar \partial_t] U(t) \Phi_\beta(x) \\ &= E_\alpha \delta_{\alpha\beta} - i\hbar \langle \Phi_\alpha | U^\dagger(t) \partial_t U(t) | \Phi_\beta \rangle. \end{aligned} \quad (51)$$

By inserting Eq. (48), we get

$$i\hbar U^\dagger(t)\partial_t U(t) = -\frac{\hbar}{2}\partial_t\theta\begin{pmatrix} 0 & -i \\ i & 0 \end{pmatrix}. \quad (52)$$

By truncating to the Andreev level subspace, we have the Hamiltonian

$$H = \begin{pmatrix} E_+ & 0 & 0 & -ig \\ 0 & E_- & ig & 0 \\ 0 & -ig & -E_+ & 0 \\ ig & 0 & 0 & -E_- \end{pmatrix}, \quad g = \frac{\hbar}{2}\partial_t\theta M. \quad (53)$$

This Hamiltonian can again be presented in a block-diagonal form, describing two equivalent two-level systems. Choosing the subspace spanned by $(\phi_+, \tilde{\phi}_-)$ and driving the magnetic field at exact resonance, $\omega = E_+ - \tilde{E}_- = E_+ + E_-$, with small amplitude, $\theta(t) = \theta_0 \sin \omega t$, where $\theta_0 \ll 1$, we have the two-level Hamiltonian,

$$H_2 = \begin{pmatrix} E_+ & -i\hbar\Omega_r \cos \omega t \\ i\hbar\Omega_r \cos \omega t & -E_- \end{pmatrix}, \quad \Omega_r = \frac{1}{2}\theta_0\omega M, \quad (54)$$

from which we obtain the Rabi oscillation of the population numbers of the ϕ representation,

$$f_+(t) = f_+(0)\cos^2\frac{\Omega_r t}{2} + [1 - f_-(0)]\sin^2\frac{\Omega_r t}{2},$$

$$[1 - f_-(t)] = [1 - f_-(0)]\cos^2\frac{\Omega_r t}{2} + f_+(0)\sin^2\frac{\Omega_r t}{2}, \quad (55)$$

or explicitly introducing the Andreev level spin,

$$f_s(t) = f_s(0) + 2S_A(0)\sin^2\frac{\Omega_r t}{2}. \quad (56)$$

This equation again illustrates the nonunitary evolution of the Andreev levels in the ϕ representation. The time evolution of the spin polarization and the Josephson current then become, respectively,

$$S_A(t) = S_A(0)\left(1 - 2\sin^2\frac{\Omega_r t}{2}\right),$$

$$I(t) = I(0) + \frac{4e}{\hbar}S_A(0)\sin^2\frac{\Omega_r t}{2}\sum_s \partial_\phi E_s. \quad (57)$$

VI. DISCUSSION

Manipulations with the Andreev levels generate strongly nonequilibrium states, whose lifetime is restricted by relaxation processes. Let us qualitatively discuss the relaxation mechanisms relevant for the nonequilibrium states induced by the discussed manipulation methods.

The phase manipulation affects the difference of the populations of the Andreev levels belonging to the same Nambu representation while keeping the total population of the Andreev level pair unchanged. At zero temperature and for rela-

tively small frequency of the qubit rotation compared to the superconducting gap, the states of the continuum spectrum are either empty or fully occupied, and therefore, the exchange between the continuum and the Andreev levels is exponentially weak.⁷ Therefore, the relaxation predominantly occurs within the Andreev level system. In the strong ZE regions, the interlevel relaxation caused by interaction with electromagnetic environment should be suppressed due to the vanishing transition matrix element [Eq. (20)], i.e., for the same reason that prevents the phase manipulation. One may expect to prolong lifetime of the excited states by taking advantage of this property and by adiabatically shifting the phase bias into the strong ZE region after the manipulation has been performed. Such an operation, however, requires a passage through one of the singular points, $\varphi = 2\pi n \pm \varphi_0$, where the Andreev levels touch the continuum; at this point, the quantum state escapes in the continuum and quantum information is lost.

The absence of the interlevel relaxation in the strong ZE regions has interesting implications for the observation of 4π periodicity of the Andreev level spectrum, as discussed in Sec. III. The equilibrium Josephson current [Eq. (15)] is 2π periodic and does not reveal the 4π -periodicity property of the Andreev states. This may change under nonequilibrium condition, when a small voltage is applied to the junction. In this case, superconducting phase becomes time dependent, $\varphi = 2eV/\hbar$, and the Andreev levels adiabatically move along the φ axis, keeping a constant level population during a long time (limited by a weak level-continuum quasiparticle exchange). If the magnetic effect is weak while contact is transparent, $\sin(\beta/2) < \sqrt{D}$, the levels touch the continuum every Josephson cycle, and the level population will be periodically reset,²⁷ leading to the 2π periodicity of the Josephson current. However, in the cigars regime, $\sin(\beta/2) > \sqrt{D}$, as depicted in Fig. 3, the levels are isolated from the continuum, and the level population may remain unchanged during the time greatly exceeding the Josephson period. This will lead to the 4π periodicity of the ac Josephson current and could be experimentally detected by observing anomalous Shapiro effect with only even Shapiro steps present. The effect would be the most pronounced for the π junctions, $\beta = \pi$. A similar effect has been discussed in a different context of unconventional superconductor junctions.³¹

Manipulation with the Andreev level spin affects the spin polarization of the Andreev levels, and thus, at first glance, a relevant relaxation mechanism would require some spin active scattering. Since the magnetic interactions in superconductors are usually rather small compared to nonmagnetic interactions, e.g., with electromagnetic environment, one would expect a long lifetime of Andreev spin excitations.⁸ However, one should take into account the relation between the spin polarization and population of the Andreev level pair Eq. (B9): The nonequilibrium spin polarization is associated with nonequilibrium population of the Andreev level pair, which can be relaxed by any nonmagnetic interaction. Consider, for example, the process of approaching the equilibrium state in magnetic contact after the phase bias has been suddenly changed. This will first create a nonequilibrium state in the Andreev level system, both in terms of individual level populations, and the total population of the level pair,

which then will rapidly relax to local equilibrium via the interlevel, and level-continuum quasiparticle transitions induced by (presumably) strong nonmagnetic interaction.⁷ Such an interaction does not change the total spin polarization of contact electrons since it preserves the spin rotation symmetry; however, it is able to transfer the polarization from the Andreev levels to the continuum states. The total polarization is maintained in the local equilibrium by shifting the energy argument in the Fermi distribution function by an energy independent constant. This constant will slowly relax to the zero value in a second relaxation stage due to spin-flip processes.

Thus, we conclude that decoherence of the states generated by the magnetic manipulations basically results from the same physical interactions that destroy excited states produced by the phase manipulations, and therefore, one should not expect significant differences of the respective lifetimes.

VII. CONCLUDING REMARKS

In conclusion, we studied the properties of Andreev bound level system and various ways of manipulation with them in Josephson quantum point contacts containing magnetic scatterers. In practice, such contacts can be realized by attaching magnetic nanoparticles or molecules to the contact bridge;²² another possibility is to insert magnetic macromolecules, e.g., doped metallofullerene, in the contact.²³ Coulomb blockade regime in molecular dots offers additional possibility due to the uncompensated spin of odd electronic configurations on the dot.^{1-3,15}

In the studied cases of resonant driving the superconducting phase difference and the direction of magnetic scatterer, the contact response consists of a time oscillation of the Josephson current, and for the magnetic drive, also oscillation of the Andreev level spin polarization. We identified the regions of external parameters, where these oscillations can be excited. The corresponding selection rule results from specific symmetry properties of the bound Andreev states in magnetic contacts: 4π periodicity of the level spectrum and strong spontaneous spin polarization.

In all of the studied cases, the nonstationary contact response results from resonant dynamics of two physically identical two-level systems (for one conducting mode), whose evolutions mirror each other. This is the manifestation in a nonstationary regime of the redundancy (double counting) of the four-component Nambu description of the Josephson effect in magnetic contacts. Due to the fundamental constraint [Eq. (7)], which is imposed by the singlet pairing, the four-component Nambu field possesses the algebraic structure of Majorana fermion,³² thus describing only 2 physical degrees of freedom rather than 4. In contacts with magnetic impurities under discussion, these 2 physical degrees of freedom relevant for the stationary Josephson effect correspond to the two Andreev bound states per conducting mode, which is similar to the case of nonmagnetic contacts.³³⁻³⁵

ACKNOWLEDGMENTS

This work was supported by the Swedish Research Coun-

cil and by the SSF-OXIDE Consortium. We are thankful to M. Fogelström and T. Löfwander for useful discussions.

APPENDIX A: BOUND STATE WAVE FUNCTIONS

To explicitly construct the wave functions of the Andreev states, we consider a quasiclassical approximation for $\phi(x)$ by separating rapidly oscillating factors $e^{\pm ik_F x}$ and slowly varying envelopes $\phi^\pm(x)$,

$$\phi(x) = \phi^+(x)e^{ik_F x} + \phi^-(x)e^{-ik_F x}. \quad (\text{A1})$$

The envelopes ϕ_v^\pm satisfy a quasiclassical Bogoliubov-de Gennes (BdG) equation,³⁶

$$i\hbar\partial_t\phi^\pm = \left(\pm v_F\hat{p}\sigma_z + \frac{\hbar}{2}\partial_x\varphi\sigma_z + \Delta\sigma_x e^{-i\sigma_z\varphi\text{sgn } x/2} \right) \phi^\pm. \quad (\text{A2})$$

Furthermore, the superconducting phase can be eliminated from this equation and moved to the boundary condition by means of the gauge transformation, $\phi \rightarrow \exp(i\sigma_z\varphi\text{sgn } x/4)\phi$.

The boundary condition at the contact for the quasiclassical envelopes, $\phi_v^\pm(0)$, follows from the electronic transfer matrix in Eq. (3). For simplicity, we assume the short contact limit, $L \ll \xi_0$, where ξ_0 is the superconducting coherence length, thus neglecting the energy dispersion of the scattering amplitudes. Then, it is easy to establish that the transfer matrix for holes has the same form as that for the electrons. Thus, the boundary condition connecting the left (L) and right (R) electrode wave functions can be written in the form

$$\begin{pmatrix} \phi^+ \\ \phi^- \end{pmatrix}_L = e^{i\sigma_z(\varphi/2)} T_e \begin{pmatrix} \phi^+ \\ \phi^- \end{pmatrix}_R. \quad (\text{A3})$$

Elementary solutions to a stationary BdG equation, $(\pm v_F\hat{p}\sigma_z + \Delta\sigma_x)\phi^\pm = E\phi^\pm$, have the form for given energy $|E| < \Delta$,

$$\phi_\alpha^\pm(x) = \frac{1}{\sqrt{2}} \begin{pmatrix} e^{\pm i\alpha\gamma/2} \\ e^{\mp i\alpha\gamma/2} \end{pmatrix} e^{-\alpha(\zeta/\hbar v_F)x}, \quad \alpha = \pm, \quad (\text{A4})$$

where

$$\cos \gamma = \frac{E}{\Delta}, \quad \sin \gamma = \frac{\zeta}{\Delta}, \quad \zeta = \sqrt{\Delta^2 - E^2}. \quad (\text{A5})$$

Index α is defined by the zero boundary condition at infinity. The matching condition [Eq. (A3)] then reads

$$\begin{pmatrix} A^+\phi^+ \\ A^-\phi^- \end{pmatrix}_{\alpha=-} = e^{i\sigma_z(\varphi/2)} T \begin{pmatrix} B^+\phi^+ \\ B^-\phi^- \end{pmatrix}_{\alpha=+}, \quad (\text{A6})$$

where the coefficients A^\pm, B^\pm are to be determined by this equation and the normalization condition. The solvability of this matching requires

$$\cos(2\gamma + \beta) = R + D \cos \varphi, \quad (\text{A7})$$

where $R = r_\uparrow r_\downarrow$ and $D = d_\uparrow d_\downarrow$ play the role of effective spin-symmetric reflection and transmission coefficients¹¹ (cf. Ref. 37 where a more general form of this equation has been

derived). By introducing a phase η through the relation, $\cos 2\eta = R + D \cos \varphi$, we obtain a solution for the quantity γ ,

$$\gamma_s = s\eta - \frac{\beta}{2} + \pi n_s, \quad s = \pm, \quad (\text{A8})$$

from which the energies of the Andreev bound states are found,

$$E_s = \theta_s \Delta \cos(s\eta - \beta/2), \quad \theta_s = \text{sgn}[\sin(s\eta - \beta/2)]. \quad (\text{A9})$$

The factor $\theta_s = \pm 1$ is fixed for each state by the condition $\sin \gamma > 0$, which guarantees the exponential decay of the bound state wave functions into the superconducting leads. To simplify the further discussion, we assume the absence of spin selection, $d_\uparrow = d_\downarrow$, $r_\uparrow = r_\downarrow$. In this case, the relation $D + R = 1$ holds, and the parameter η can be chosen as follows:

$$\sin \eta = \sqrt{D} \sin \frac{\varphi}{2}. \quad (\text{A10})$$

To write down an explicit form of the Andreev level wave functions, it is convenient to combine the envelopes [Eq. (A1)] in a four vector $\hat{\phi}_s = (\phi_s^+, \phi_s^-)$, then

$$\hat{\phi}_s(x > 0) = \begin{pmatrix} v_s & 0 \\ 0 & v_s^* \end{pmatrix} \begin{pmatrix} F_s \\ i\theta_s F_{-s} \end{pmatrix} G_s(x), \quad (\text{A11})$$

$$\hat{\phi}_s(x < 0) = s\theta_s \begin{pmatrix} -\sigma_x & 0 \\ 0 & \sigma_x \end{pmatrix} \hat{\phi}_s(x > 0), \quad (\text{A12})$$

where

$$v_s = \frac{1}{\sqrt{2}} \begin{pmatrix} e^{i\gamma_s/2} \\ e^{-i\gamma_s/2} \end{pmatrix}, \quad (\text{A13})$$

and

$$F_s = \sqrt{\varepsilon - s\sqrt{D} \cos \frac{\varphi}{2}},$$

$$G_s(x) = \sqrt{\frac{\zeta_s}{2\hbar v_F \varepsilon}} e^{-(\zeta_s/\hbar v_F)|x|},$$

$$\varepsilon = \sqrt{1 - D \sin^2(\varphi/2)}. \quad (\text{A14})$$

APPENDIX B: SYMMETRY RELATIONS

The symmetry relation [Eq. (7)] generates the relations between the density matrices ρ and $\tilde{\rho}$,

$$\tilde{\rho}(x, x', t) = \delta(x - x') - (i\sigma_y) \rho^*(x, x', t) (i\sigma_y)^\dagger, \quad (\text{B1})$$

which extends to the respective single particle Hamiltonians by virtue of the Liouville equation,

$$\tilde{h} = -(i\sigma_y) h^* (i\sigma_y)^\dagger. \quad (\text{B2})$$

Furthermore, Eq. (B2) generates the symmetry relation between the respective eigenstates,

$$\tilde{\phi}_\nu(x) = (i\sigma_y) \phi_\nu^*(x), \quad (\text{B3})$$

and eigenenergies,

$$\tilde{E}_\nu = -E_\nu. \quad (\text{B4})$$

Equations (B3) and (B4) establish mapping between the Hilbert spaces of the reciprocal Nambu representations, i.e., ϕ representation and $\tilde{\phi}$ representation. The eigenstates of these representations form complete orthogonal sets, $\langle \phi_\nu, \phi_{\nu'} \rangle = \langle \tilde{\phi}_\nu, \tilde{\phi}_{\nu'} \rangle = \delta_{\nu\nu'}$. Furthermore, they obey an additional orthogonality relation,

$$\langle \phi_\nu, \tilde{\phi}_{\nu'} \rangle = 0, \quad (\text{B5})$$

which straightforwardly follows from the local identity, $[\phi_\nu(x), i\sigma_y \phi_\nu^*(x)] = 0$; the brackets here denote a scalar product of two vectors.

The matrix elements of the reciprocal density matrices, $\rho(x, x', t)$ and $\tilde{\rho}(x, x', t)$, in the respective eigenbases [cf. Eq. (13)],

$$\rho_{\nu\nu'}(t) = \langle \phi_{\nu'}, \rho(t) \phi_\nu \rangle, \quad \tilde{\rho}_{\nu\nu'}(t) = \langle \tilde{\phi}_{\nu'}, \tilde{\rho}(t) \tilde{\phi}_\nu \rangle, \quad (\text{B6})$$

obey the symmetry relation,

$$\tilde{\rho}_{\nu\nu'} = \delta_{\nu\nu'} - \rho_{\nu\nu'}^*. \quad (\text{B7})$$

In particular, the relation between the population numbers, $f_\nu = \rho_{\nu\nu}$ and $\tilde{f}_\nu = \tilde{\rho}_{\nu\nu}$, reads

$$\tilde{f}_\nu = 1 - f_\nu. \quad (\text{B8})$$

The Andreev charge current and spin polarization are identical in both representations,

$$I_A = \frac{e}{\hbar} \sum_{s=\pm} \partial_\varphi E_s (1 - 2f_s) = \frac{e}{\hbar} \sum_{s=\pm} \partial_\varphi \tilde{E}_s (1 - 2\tilde{f}_s),$$

$$S_A = \frac{1}{2} (1 - f_+ - f_-) = -\frac{1}{2} (1 - \tilde{f}_+ - \tilde{f}_-). \quad (\text{B9})$$

¹J. A. van Dam, Y. V. Nazarov, E. P. A. M. Bakkers, S. De Franceschi, and L. P. Kouwenhoven, *Nature (London)* **442**, 667 (2006).

²H. I. Jørgensen, K. Grove-Rasmussen, T. Novotný, K. Flensberg, and P. E. Lindelof, *Phys. Rev. Lett.* **96**, 207003 (2006).

³J.-P. Cleuziou, W. Wernsdorfer, V. Bouchiat, T. Ondarcuhu, and M. Monthieux, *Nat. Nanotechnol.* **1**, 53 (2006).

⁴V. S. Shumeiko, G. Wendin, and E. N. Bratus', *Phys. Rev. B* **48**, 13129 (1993).

⁵L. Y. Gorelik, V. S. Shumeiko, R. I. Shekhter, G. Wendin, and M.

- Jonson, Phys. Rev. Lett. **75**, 1162 (1995).
- ⁶A. Zazunov, V. S. Shumeiko, E. N. Bratus', J. Lantz, and G. Wendin, Phys. Rev. Lett. **90**, 087003 (2003).
- ⁷A. Zazunov, V. S. Shumeiko, G. Wendin, and E. N. Bratus', Phys. Rev. B **71**, 214505 (2005).
- ⁸N. M. Chtchelkatchev and Yu. V. Nazarov, Phys. Rev. Lett. **90**, 226806 (2003).
- ⁹M. Fogelström, Phys. Rev. B **62**, 11812 (2000).
- ¹⁰J. C. Cuevas and M. Fogelström, Phys. Rev. B **64**, 104502 (2001).
- ¹¹Yu. S. Barash and I. V. Bobkova, Phys. Rev. B **65**, 144502 (2002).
- ¹²Yu. S. Barash, I. V. Bobkova, and T. Kopp, Phys. Rev. B **66**, 140503(R) (2002).
- ¹³E. V. Bezuglyi, A. S. Rozhavsky, I. D. Vagner, and P. Wyder, Phys. Rev. B **66**, 052508 (2002).
- ¹⁴Z. Radovic, N. Lazarides, and N. Flytzanis, Phys. Rev. B **68**, 014501 (2003).
- ¹⁵E. Vecino, A. Martín-Rodero, and A. Levy Yeyati, Phys. Rev. B **68**, 035105 (2003).
- ¹⁶I. Petkovic, N. M. Chtchelkatchev, and Z. Radovic, Phys. Rev. B **73**, 184510 (2006).
- ¹⁷C. Benjamin, T. Jonckheere, A. Zazunov, and T. Martin, Eur. Phys. J. B **57**, 279 (2007).
- ¹⁸J.-X. Zhu and A. V. Balatsky, Phys. Rev. B **67**, 174505 (2003).
- ¹⁹J.-X. Zhu, Z. Nussinov, A. Shnirman, and A. V. Balatsky, Phys. Rev. Lett. **92**, 107001 (2004).
- ²⁰L. Bulaevskii, M. Hruška, A. Shnirman, D. Smith, and Yu. Makhlin, Phys. Rev. Lett. **92**, 177001 (2004).
- ²¹Z. Nussinov, A. Shnirman, D. P. Arovas, A. V. Balatsky, and J.-X. Zhu, Phys. Rev. B **71**, 214520 (2005).
- ²²W. Wernsdorfer, E. B. Orozco, K. Hasselbach, A. Benoit, B. Barbara, N. Demoncy, A. Loiseau, H. Pascard, and D. Mailly, Phys. Rev. Lett. **78**, 1791 (1997).
- ²³A. Yu. Kasumov, K. Tsukagoshi, M. Kawamura, T. Kobayashi, Y. Aoyagi, K. Senba, T. Kodama, H. Nishikawa, I. Ikemoto, K. Kikuchi, V. T. Volkov, Yu. A. Kasumov, R. Deblock, S. Guéron, and H. Bouchiat, Phys. Rev. B **72**, 033414 (2005).
- ²⁴A. Altland and M. R. Zirnbauer, Phys. Rev. B **55**, 1142 (1997).
- ²⁵E. Zhao, T. Löfwander, and J. A. Sauls, Phys. Rev. B **70**, 134510 (2004).
- ²⁶Y. Nambu, Phys. Rev. **117**, 648 (1960).
- ²⁷L. Y. Gorelik, N. I. Lundin, V. S. Shumeiko, R. I. Shekhter, and M. Jonson, Phys. Rev. Lett. **81**, 2538 (1998).
- ²⁸I. O. Kulik, Zh. Eksp. Teor. Fiz. **49**, 1211 (1965) [Sov. Phys. JETP **22**, 841 (1966)].
- ²⁹The spin current of the continuum spectrum states is zero in the equilibrium, as can be shown by straightforward calculation.
- ³⁰J. Lantz, V. S. Shumeiko, E. N. Bratus', and G. Wendin, Physica C **368**, 315 (2002).
- ³¹H.-J. Kwon, K. Sengupta, and V. M. Yakovenko, Eur. Phys. J. B **37**, 349 (2004).
- ³²J. Fuchs and C. Schweigert, *Symmetries, Lie Algebras and Representations* (Cambridge University Press, Cambridge, 2003), p. 350.
- ³³A. Furusaki and M. Tsukada, Physica B (Amsterdam) **165-166**, 967 (1990); Phys. Rev. B **43**, 10164 (1991).
- ³⁴C. W. J. Beenakker and H. van Houten, Phys. Rev. Lett. **66**, 3056 (1991).
- ³⁵S. V. Sharov and A. D. Zaikin, Phys. Rev. B **71**, 014518 (2005).
- ³⁶V. Shumeiko, E. Bratus, and G. Wendin, Low Temp. Phys. **23**, 181 (1997).
- ³⁷G. Wendin and V. S. Shumeiko, Superlattices Microstruct. **20**, 569 (1996).